Exp Brain Res (2006) 173: 724–732
DOI 10.1007/s00221-006-0447-1

RESEARCH ARTICLE

Scott A. Beardsley · Lucia M. Vaina

Global motion mechanisms compensate local motion deficits in a patient with a bilateral occipital lobe lesion

Received: 9 November 2005 / Accepted: 14 March 2006 / Published online: 4 May 2006

Abstract Successive stages of cortical processing encode increasingly more complex types of information. In the visual motion system this increasing complexity, complemented by an increase in spatial summation, has proven effective in characterizing the mechanisms mediating visual perception. Here we report psychophysical results from a motion-impaired stroke patient, WB, whose pattern of deficits over time reveals a systematic shift in spatial scale for processing speed. We show that following loss in sensitivity to low-level motion direction WB's representation of speed shifts to larger spatial scales, consistent with recruitment of intact high-level mechanisms. With the recovery of low-level motion processing WB's representation of speed shifts back to small spatial scales. These results support the recruitment of high-level visual mechanisms in cases where lower-level function is impaired and suggest that, as an experimental paradigm, spatial summation may provide an important avenue for investigating functional recovery in patients following damage to visually responsive cortex.

Keywords Complex motion · Neurological patient · Optic flow · Psychophysics · Visual motion deficits · Neuropsychology

S. A. Beardsley
Department of Biomedical Engineering, Marquette University, Milwaukee, WI, USA

L. M. Vaina (✉)
Department of Biomedical Engineering, Boston University, Boston, MA, USA
E-mail: vaina@bu.edu
Tel.: +1-617-3532455
Fax: +1-617-3580731

L. M. Vaina
Department of Neurology, Harvard Medical School, Boston, MA, USA

Introduction

Psychophysical studies of complex motion processing indicate that speed and direction are processed at different cortical levels in the human brain. Direction discrimination is processed at large spatial scales by specialized detectors for radial, circular, and spiral motions (Morrone et al. 1995; Burr et al. 1998; Beardsley and Vaina 2001; Meese and Harris 2001; Meese and Anderson 2002; Beardsley and Vaina 2004; Beardsley and Vaina 2005b) that integrate local motions across the visual field to obtain a global motion percept (Morrone et al. 1995; Burr et al. 1998). Speed discrimination, by contrast, is computed locally over small spatial scales. Several studies have demonstrated that speed discrimination in coherent radial or circular motions is not significantly different from stimuli containing planar or random motion (Sekuler 1992; Bex et al. 1998; Clifford et al. 1999), suggesting a simple pooling process across elementary detectors for motion direction (Sekuler 1992; Clifford et al. 1999).

The use of elementary motion detectors to process changes in the speed of complex motions is somewhat surprising given the role of radial and circular motion mechanisms in comparing speeds between *different* types of complex motion (Geesaman and Qian 1996; Bex and Makous 1997; Bex et al. 1998; Geesaman and Qian 1998). The spatial summation of local motion signals inherent to radial and circular motion mechanisms would seem to make them better suited to detect small changes in the speed of wide-field radial and circular motions.

Current theories of selective attention (Usher and Niebur 1996; Deco and Zihl 2001; Hahnloser et al. 2002; Deco and Rolls 2004) and perceptual learning (Hochstein and Ahissar 2002; Ahissar and Hochstein 2004) support this view, suggesting a more direct role for mechanisms encoding large scale features relevant to a task. In both cases processing has been proposed to occur at the highest cortical level whose output is discriminative with respect to the task. Under these conditions complex

(radial and circular) motion mechanisms and not motion direction mechanisms should dominate the speed percept.

The spatially localized nature of speed processing suggests that the brain instead attempts to identify the lowest cortical level *sufficient* to perform the task. Thus, when low level processing becomes insufficient following a loss in sensitivity as a result of stroke or aging for example, the visual system may recruit higher cortical levels that maintain sensitivity by integrating motion signals across space and/or time. This integration process, referred to as spatial (or temporal) summation, reduces the impact of low-level noise by averaging across multiple inputs at the expense of a coarser spatial or temporal resolution in the output. In the case of speed, the recruitment of higher-level complex motion mechanisms seems reasonable given the increased spatial summation observed at successively later stages of visual motion processing.

In a recent study Vaina et al. (2003) reported on a patient, AMG, whose ability to process wide field planar motion was robust to impairment in the low-level encoding of motion information. Utilizing a battery of visual motion tasks they demonstrated that the spatial and temporal summation properties of higher-level mechanisms were sufficient to offset low-level visual motion deficits. While the study did not explicitly indicate recruitment of high-level mechanisms to perform low-level motion tasks, it suggests that recruitment could occur in cases where visual motion properties spanning multiple spatial scales are initially processed at small spatial scales.

Here, we report psychophysical results from a motion-impaired stroke patient, WB, whose pattern of spatial summation over time supports the recruitment of intact radial motion mechanisms to discriminate speed following impairment of elementary motion detectors. Using spatial summation as an experimental paradigm, we demonstrate systematic shifts in WB's representation of motion direction and speed to later stages of processing whose increased spatio-temporal integration could be used to offset local motion deficits. In the case of speed discrimination we show that this was later followed by a shift back to the use of local motion mechanisms and functional recovery on the task.

Methods

Apparatus

All stimuli were presented on a 17-in. Apple Studio Display monitor set to an 832×624 resolution and 75 Hz refresh rate. The display was set to a calibrated 8-bit gray-scale mode and controlled by a 400 MHz PowerMac G4 running OS 9. The stimuli and tests were developed using C in conjunction with the Video toolbox (Pelli 1997) and MacGLib 2.0 (Micro ML Inc., Québec, Canada) programming libraries. All displays were viewed binocularly at a distance of 56 cm in a darkened room.

Stimuli

Stimuli were random dot kinematograms (RDKs) containing either expanding or contracting dot motion relative to the stimulus center (Fig. 1a). Each RDK contained 406 dots (0.95 dots/deg^2; 22.01 Cd/m^2) presented on a gray background (13.7 Cd/m^2). Dots were presented in a 24° diameter annular aperture (central 4° removed) whose borders were illusory as defined by an absence of dots. RDK motion sequences were generated off-line and presented for 440 ms with a 500 ms interstimulus interval.

At the subject viewing distance each 4×4 pixel dot subtended 9.8 min of visual angle and moved through a radial speed gradient whose average speed was 8.4 deg/s, with a maximum speed of 12.3 deg/s at the outer aperture. Dots were presented with a fixed lifetime of 11 frames (147 ms) uniformly distributed across the first 11 frames of the stimulus. Constant dot density was maintained by pseudo-randomly repositioning dots that moved beyond the aperture to regions of the display depopulated by the dot motion (Clifford et al. 1999). Timing-based judgments were minimized by perturbing the duration of each stimulus (440±40 ms).

Spatial summation

In the experiments outlined below, spatial summation was examined by systematically masking regions of the display. The stimulus was subdivided into 'signal' sectors, containing dot motion, and blank masking sectors set to background luminance. Dot density at the boarders was maintained by internally updating the positions of dots located in the masked and unmasked regions of the display. Those dots whose locations fell within unmasked sectors were then drawn to the display.

Spatial summation was examined using three stimulus configurations to control for visual field asymmetries in the patient (Fig. 1b). In the multi-sector condition the stimulus was divided into 16 equal sectors (width =22.5°). Subjects were tested with stimuli containing 1, 2, 4, 8, or 16 signal sectors whose locations were maximally separated in the display. In the second condition a single signal sector centered on the horizontal axis was presented at each of five widths (22.5, 45, 90, 180, or 360°). The third condition consisted of a single signal sector oriented at 308°, corresponding to the region of maximal visual field sparing in the patient. Up to 22 sector widths were tested spanning the range from 30 to 360° (15° intervals) to quantify spatial recruitment.

Procedure

Prior to the start of an experimental session, observers adapted to the background luminance of the monitor display in a quiet darkened room. During testing,

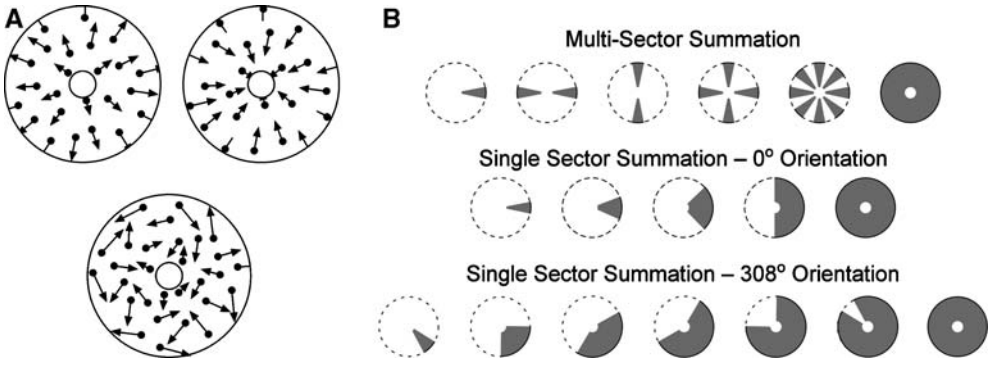

Fig. 1 Schematic representation of the stimuli used in the direction and speed discrimination experiments. **a** In each experiment limited-lifetime dots moved along fixed trajectories either towards (*contraction*) or away (*expansion*) from the center of the stimulus aperture (*top*). In a separate control condition, speed discrimination was also tested with a random walk stimulus consisting of dots whose trajectories were randomly chosen after each frame (*bottom*). Dot speed was proportional to the distance from the stimulus center with a mean speed of 8.4 deg/s, **b** spatial summation masks used in each experiment. The *dashed line* denotes the outer stimulus aperture. *Filled regions* indicate 'signal' sectors containing dot motion. Masked regions (*white*) contained no dots and were set to the background luminance of the display

subjects were required to fixate a small central square (11×11 pixels; 22.01 Cd/m^2). An attending auditory trigger preceded each stimulus presentation. At the end of the trial subjects were required to make a judgment by pressing a key, after which the next trial was presented. Adaptation to specific directions of motion was minimized by randomly interleaving presentation of expanding and contracting motions across trials.

An adaptive staircase procedure was used to determine the threshold at which subjects could discriminate differences in direction (experiment 1) or speed (experiment 2) with 79% probability. Each staircase started at supra-thresholds levels (i.e., 100% coherence or speed difference) and contained 96 equally spaced levels spanning three log units of coherence or speed difference, respectively. Testing proceeded using a one down, one up design with decreasing step size. Initial step size was set to nine staircase levels to quickly estimate the threshold region and was systematically decreased to six, four, and two staircase levels following each of the first three reversals. After the fourth reversal, step size was set to one and the staircase switched to a three down, one up design to obtain an estimate of threshold. Testing was stopped after ten reversals and discrimination thresholds were estimated as the mean across the last six reversals. The width and number of masking sectors were counterbalanced across staircase sessions.

In one experimental condition (single- and multi-sector summation 15 months post lesion) WB's ability to discriminate direction (experiment 1) was assessed using a constant stimulus design. In this case, eight constant stimulus levels spanning the range from 15 to 100% coherence were presented for each sector mask configuration. Stimuli were presented in pseudo-random order with each constant stimulus level presented 20 times. For each type of stimulus mask a two-parameter least-squares Weibull fit to the resulting psychometric function was used to estimate threshold. As with the staircase design, discrimination thresholds were calculated as the proportion of signal dots necessary to discriminate radial motion direction with 79% probability.

Observers

Patient WB is a 65-year-old right-handed man who suffered an infarct in the territory of the posterior cerebral artery (PCA) bilaterally, resulting in a large scotoma with foveal sparing (central ±10°), and with sparing of a wedge of roughly 40° in the right inferior quadrant (Fig. 2). In the left upper field there was a small sparing as well. The lesion in the left hemisphere involved the occipital and medial temporal area and the inferior calcarine cortex. In the right hemisphere, the calcarine cortex was also involved with sparing of the inferio-lateral portion. The occipital pole was spared in both left and right hemispheres.

WB was studied in our laboratory with a variety of visual motion tasks during three 1-week long visits. During each visit he participated in daily psychophysical examinations lasting several hours but with frequent breaks. WB's ability to fixate was documented through Humphrey perimetry and during testing stimulus fixation was monitored visually by the examiner. In all experimental conditions stimuli were presented in the central 24° of WB's intact foveal field (Fig. 2—red circles). The patient was very motivated and was able to maintain good fixation throughout the duration of each test.

In addition to patient WB, 12 normal right-handed observers participated in the psychophysical tasks. All observers had normal or corrected to normal vision. Two observers participated in both experiments. Of the remaining ten, six participated in the motion pattern coherence task (experiment 1) and four participated in the speed discrimination task (experiment 2). With the exception of one of the authors, SB, all observers were naïve to the purpose of the experiments. Prior to their

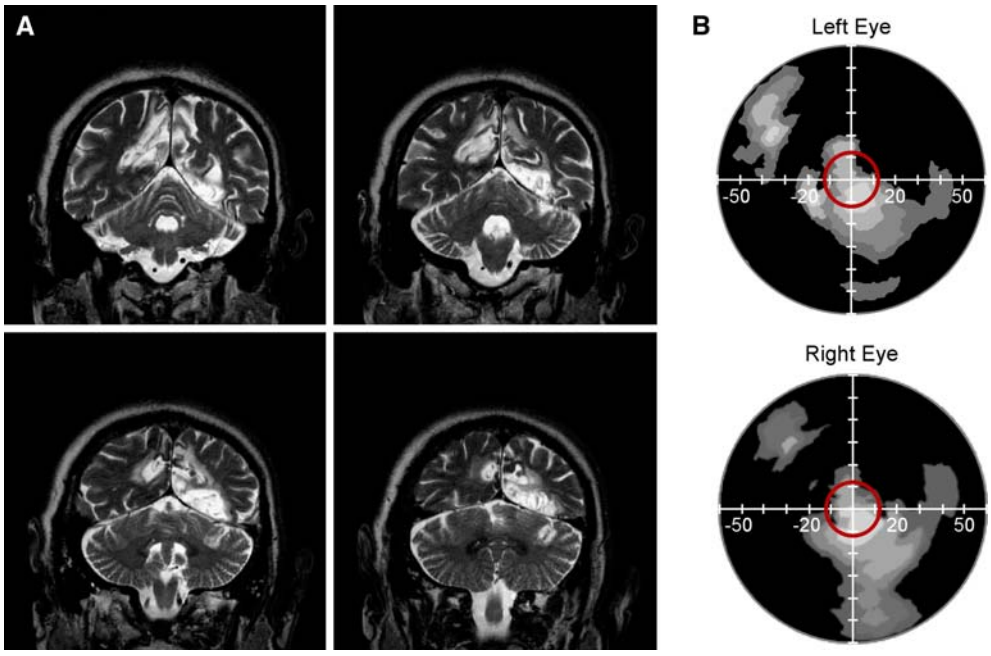

Fig. 2 **a** Coronal T1-weighted MR slices illustrating WB's lesion (shown in *white*). In the left hemisphere the lesion involved the occipital and medial temporal area and the inferior calcarine cortex. In the right hemisphere, the calcarine cortex was also involved with sparing of the inferio-lateral portion. The occipital pole was spared in both *left* and *right* hemispheres. **b** Visual fields of WB following the stroke. Humphrey perimetry revealed a large scotoma with foveal sparing (central ±10°), and with sparing of a wedge of roughly 40° in the right inferior quadrant. WB's visual fields remained stable during his participation in the study. In all experimental conditions stimuli were presented in the central 24° of WB's intact visual field centered on the fovea (*red circles*)

participation in the study written informed consent was obtained from all subjects in accordance with Boston University's Institutional Review Board Committee on research involving human subjects, the Declaration of Helsinki, and the NIH regulations regarding the use of human subjects in research.

Results

Experiment 1: motion pattern coherence

In a single interval task WB was required to discriminate the direction of radial motion (expansion versus contraction) formed by a proportion of coherently moving 'signal' dots in the display. Dots were randomly assigned as 'signal' or 'noise' on a frame-by-frame basis such that signal dots moved in directions consistent with the radial motion being presented and noise dots were repositioned at random locations within the stimulus aperture (Fig. 1a).

The effect of stimulus area on WB's performance was examined over the course of 11 months using three types of stimulus mask to control for visual field asymmetries (Fig. 1b). For each mask, motion coherence thresholds were measured as the proportion of signal dots necessary to discriminate the direction of radial motion in the display. Between one and four thresholds were obtained for each stimulus condition.

Figure 3 shows WB's performance as a function of stimulus area for three test sessions performed 15, 18, and 26 months after the infarct. At 15 months, coherence thresholds were normal (Fig. 3a, b). Thresholds were robust to differences in the type of stimulus mask and were well fit by a linear regression on a log–log scale ($r^2 > 0.87$). For both stimulus masks, thresholds decreased with the square-root of stimulus area ($|\gamma| = 0.5$) as measured by the regression slope ($|\gamma| = 0.47 \pm 0.12$ and 0.46 ± 0.14 for multi- and single-sector masks, respectively). Performance was similar at 18 and 26 months. In all cases, WB's thresholds and the extent of summation were well matched to normal control observers.

The decrease in WB's coherence thresholds with the square-root of stimulus area is consistent with predictions of an ideal observer that uses a range of visual motion filters matched in extent to the stimulus areas tested (Morrone et al. 1995; Burr et al. 1998; Tyler and Chen 2000). This agrees well with previous studies of spatial summation in complex motion stimuli (Morrone et al. 1995; Burr et al. 1998) and suggests that WB's performance on the task was mediated by mechanisms specifically sensitive to radial motion direction across large spatial scales.

By comparison, WB's coherence thresholds for small field (10° diameter; 78.5 deg^2) planar motions (0.78 ± 0.14) were significantly worse than normal control observers (0.12 ± 0.04, $n = 12$) at 15 months but not at 26 months (0.11 ± 0.05), (Fig. 4a). WB's initial dissociation between planar and radial motion discrimination for stimuli spanning comparable spatial extent (78.5 and 54.9 deg^2, respectively) is important because it suggests impairment, not of the radial motion mechanisms, but of the motion direction mechanisms that feed into them. This interpretation is consistent with WB's inability at 15 and 18 months to discriminate radial direction in the smallest single-sector tested ($= 27.5$ deg^2, data not shown) for which motion is approximately planar. It also agrees well with computational models of complex motion processing. In such models the integration of

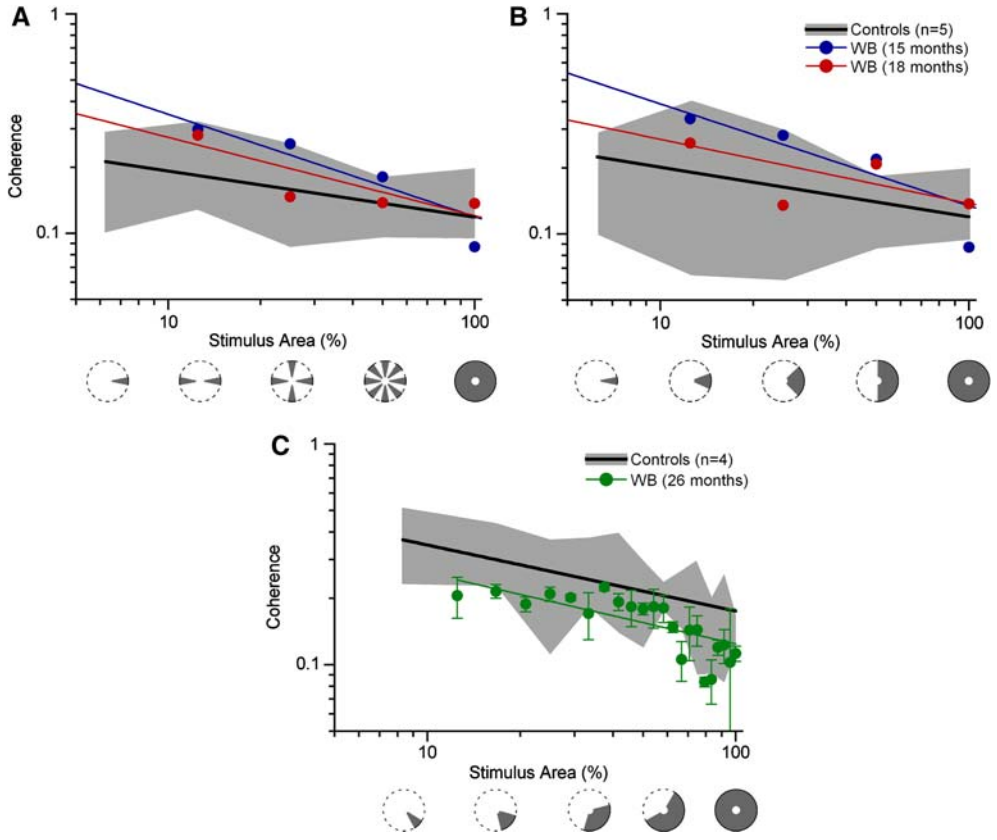

Fig. 3 Radial motion coherence as a function of stimulus area. The type of stimulus mask is indicated schematically along the abscissa. *Shaded regions* indicate the range in thresholds across normal observers (mean ± SD). Thresholds are shown at 15 (*blue*), 18 (*red*), and 26 (*green*) months after WB's lesion together with the best-fit linear regression. Error bars are ±1 SEM. The *thick black line* indicates the best-fit averaged across normal observers. **a** WB's performance was normal 15 months after the lesion. Thresholds decreased linearly with stimulus area with a slope ($|\gamma|=0.47\pm0.12$, $r^2=0.91$) that was well matched to predictions of an ideal observer ($|\gamma|=0.5$). Similar performance was obtained at 18 months ($|\gamma|=0.36\pm0.10$, $r^2=0.87$) and **b** with the single-sector mask, **c** discrimination thresholds showed a small but systematic improvement at 26 months, however, the extent of spatial summation remained unchanged ($|\gamma|=0.32\pm0.06$, $r^2=0.61$). Note that the slight change in masking paradigm shown in (**c**) did not impact the extent of WB's spatial summation

motion directions across space yields responses that are robust to loss in the number and accuracy of individual direction estimates (Hatsopoulos and Warren 1991; Perrone and Stone 1998; Zemel and Sejnowski 1998; Beardsley and Vaina 2005a).

Given the anisotropic nature of WB's visual field deficits one could argue that the increase in thresholds for small signal sectors be due to visual field loss along the horizontal mid-line and not impairment of motion direction mechanisms per se. The presentation of stimuli in WB's central spared visual field using multiple stimulus masks is designed to minimize this effect. If asymmetries in WB's intact visual field impact on performance then coherence thresholds should vary based on the configuration of the stimulus mask for stimuli spanning the same area. Specifically, thresholds between the horizontal and vertical two-sector masks (22.5° each) and the single 45°sector mask of equal area (54.9 deg^2) should be significantly different (Fig. 3a, b). Similarly, performance should vary with orientation for a single-sector. In both cases thresholds were equivalent, arguing against a primary effect of visual field asymmetries on spatial summation.

Experiment 2: speed discrimination

In a second experiment we assessed WB's ability to discriminate speed of radial motion as a function of stimulus area. Psychophysical studies in normal observers have consistently shown speed discrimination for radial motions to occur at the level of spatially localized motion direction mechanisms (Sekuler 1992; Clifford et al. 1999), although higher-level mechanisms have been implicated in the perception of speed for complex motion (Geesaman and Qian 1996; Bex and Makous 1997; Bex et al. 1998; Geesaman and Qian 1998). Given the existence of specialized detectors selective for radial, circular, and spiral motions (Morrone et al. 1995; Burr et al. 1998; Meese and Harris 2001; Meese and Anderson 2002; Beardsley and Vaina 2004; Beardsley and Vaina 2005b), it is curious that they do not play a more direct role in discriminating speed. In cases of low-level motion impairment, such as with WB, the capability of these higher-level mechanisms to encode speed suggests that the visual system could recruit them to compensate damage to early cortical levels.

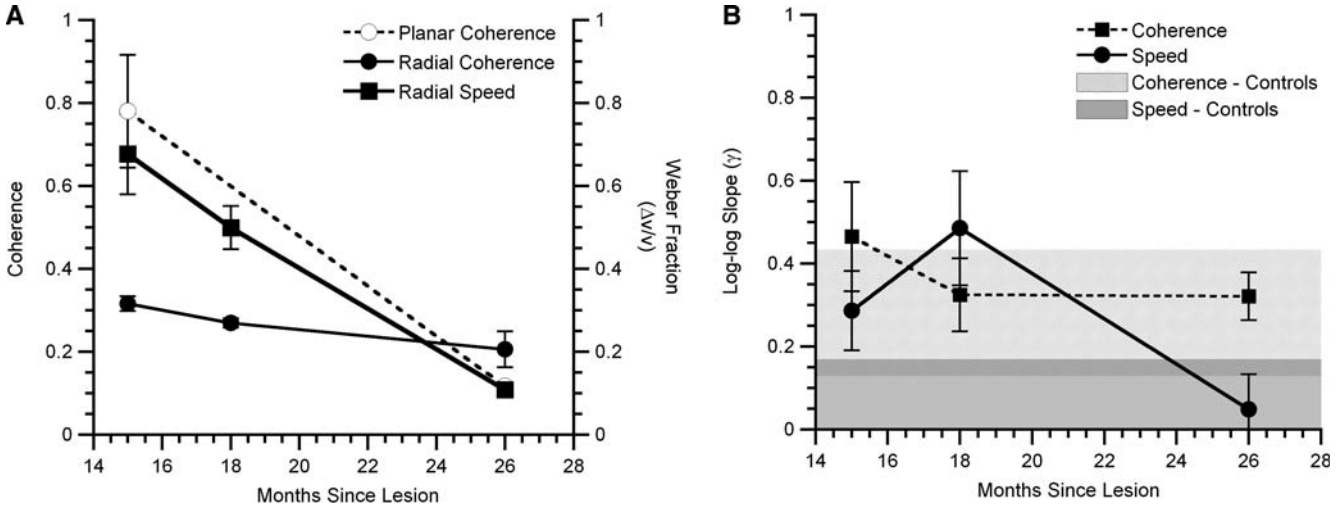

Fig. 4 Discrimination thresholds and summation slopes (γ) for WB as a function of time since the lesion. **a** Direction discrimination for planar motion (10° diameter; 78.5 deg^2) was severely impaired 15 months after the lesion and recovered by 26 months (*open circles; left ordinate*). For radial motions spanning comparable spatial extent (12.5% of total stimulus area = 54.9 deg^2), performance was normal (*filled circles*). Thresholds for radial motion decreased slightly with time, however, the change was not significant. By comparison, speed discrimination for radial motions (spanning 54.9 deg^2) was severely impaired at 15 months. Performance improved systematically with time, and was normal by 26 months, **b** the extent of WB's spatial summation on the motion coherence task (*filled squares*) was normal 15, 18, and 26 months after the lesion. Spatial summation on the speed discrimination task (*filled circles*) followed a markedly different trend during this time, first increasing to the level of an ideal observer from 15 to 18 months and then decreasing to the level of normal observers by 26 months. *Shaded regions* indicate the range in summation slopes across normal observers (mean ± SD). Error bars are ±1 SEM

In the speed discrimination task pairs of expanding or contracting motions were presented binocularly at 100% coherence in a temporal two-alternative-forced-choice paradigm. Each stimulus pair contained a comparison stimulus whose dots moved with an average speed of 8.4 deg/s and a test stimulus that moved either faster or slower. During testing the order of test and comparison stimuli were counterbalanced across trials and subjects were required to identify the stimulus interval containing the faster average dot motion. To minimize the effects of stimulus adaptation, expanding and contracting motions were randomly interleaved in a dual-staircase paradigm. Speed discrimination thresholds for radial motion corresponded to the average obtained across expanding and contracting motions.

In a separate control condition, speed discrimination was measured for stimuli containing incoherent motion (Fig. 1a). In this condition, referred to as random walk, the direction of motion was specified randomly for each dot during each frame of the motion sequence. The lack of coherent direction information limited the ability of observers to spatially integrate speed information across the display, providing an estimate of subjects' ability to discriminate speed based on differences in local motions between stimuli.

As in experiment 1, WB's ability to discriminate differences in speed was examined at 15, 18, and 26 months after the infarct. At 15 months, spatial summation was measured using both random walk and radial motion stimuli. For random walk stimuli in particular, WB's ability to discriminate speed was severely impaired. Thresholds approached a Weber fraction of 1 ($\Delta v/v = 1$) for all but the largest stimuli, exhibiting little effect of stimulus area for all but the largest stimuli ($|\gamma| = 0.21 \pm 0.18$; Fig. 5). Control observers exhibited similar trends in performance ($|\gamma| = 0.004 \pm 0.12$), albeit at much lower thresholds. In both cases the extent of spatial summation is indicative of an attentional summation mechanism (Tyler and Chen 2000), in which observers employ an ideal attention window, matched to the stimulus extent, to individually monitor changes in speed across a large number of low-level, or 'elementary', motion detectors (Sekuler 1992; Clifford et al. 1999). This result agrees well with previous studies in which speed discrimination has been shown not to exceed predictions of a simple pooling (linear summation) rule (Sekuler 1992), and in the case of WB suggests impairment among motion direction mechanisms sampling limited regions of the visual field.

Across normal observers, speed discrimination for radial motion was consistently better than for random walk. Such improvement would be expected given the increased spatio-temporal integration of velocity signals (Watamaniuk and Duchon 1992; Watamaniuk and Sekuler 1992) and is in agreement with studies contrasting speed discrimination for incoherent versus coherent complex motion (Clifford et al. 1999). However, coherent radial motion did not significantly improve discrimination for larger stimuli, resulting in little if any change in spatial summation across normal observers ($|\gamma| = 0.04 \pm 0.03$).

By comparison, WB's ability to discriminate speed improved systematically with stimulus area (Fig. 5; GLM, $t(6) = 2.68$, $p < 0.05$, one-sided). The corresponding slope ($|\gamma| = 0.29 \pm 0.09$) was slightly greater than

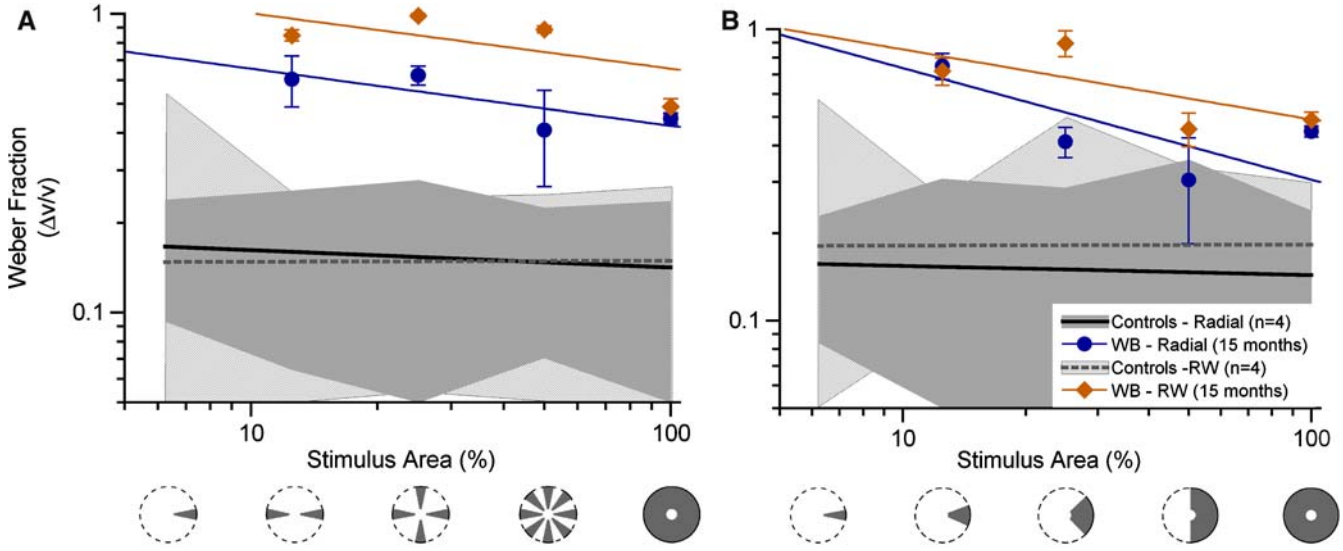

Fig. 5 Speed discrimination as a function of stimulus area 15 months after the lesion. Thresholds for random walk (*RW*; *diamonds*), and radial motion (*circles*), were obtained for (**a**) multi- and (**b**) single-sector mask conditions. All other symbols are the same as in Fig. 3. Speed discrimination was severely impaired with random walk stimuli in which spatial and temporal integration was limited. Although WB remained impaired with radial motions thresholds were consistently lower across mask conditions. The corresponding increase in summation ($|\gamma| = 0.29 \pm 0.09$) for radial motion contrasts sharply with that of normal control observers ($|\gamma| = 0.04 \pm 0.03$) for whom stimulus size had little or no effect

predictions for a simple attention summation mechanism ($|\gamma| \leq 0.25$) (Tyler and Chen 2000), suggesting a shift toward the use of larger spatial summing fields to discriminate changes in speed.

For small stimulus sectors, the equivalence between WB's ability to discriminate speed in radial motion and random walk suggests that the underlying mechanisms were not explicitly dependent on coherent motion direction. Similar effects have been shown in normal observers for fixed random trajectory stimuli (Clifford et al. 1999), and in the case of WB, suggests that speed was processed locally before significant spatial and temporal integration of motion directions occurred. By comparison, speed discrimination for full field radial motions was significantly better than for small stimulus sectors, consistent with the use of radial motion mechanisms that spatio-temporally integrate motions along complex trajectories.

At 18 months, WB's thresholds decreased for all mask conditions (Fig. 6a, b). The change in thresholds was modest for small field stimuli but increased quickly with stimulus area, reaching normal levels in the case of full field stimuli. Spatial summation increased as well during this time ($|\gamma| = 0.49 \pm 0.14$), to levels predicted by an ideal observer. This result is significant computationally in that it signals a shift in processing toward the use of increasingly larger summing fields that span the range of stimulus sizes tested (Tyler and Chen 2000).

WB's trend toward increased spatial summation changed abruptly at 26 months. At that time speed discrimination was normal for all stimulus sizes ($p > 0.05$, $t < 2.0$). The extent of spatial summation ($|\gamma| = 0.05 \pm 0.08$), was also normal suggesting a shift in processing back to the use of an attention summation mechanism operating across local motion detectors.

Discussion

In the above experiments we have demonstrated a clear pattern of visual motion deficits in a patient, WB, that indicate a dissociation between the low-level encoding of speed and direction in complex motion tasks requiring spatio-temporal integration. WB's initial impairments in discrimination of planar motion direction coupled with the increase in motion coherence thresholds (experiment 1) for radial motions masked to the smallest stimulus extent, is consistent with impairment of the motion direction mechanisms and sparing of the radial motion mechanisms to which they project. His deficits discriminating speed in radial motions and random walk stimuli (experiment 2) provide additional support for a local motion impairment distinct from the mechanisms that process radial motion direction. Similar patterns of deficits have been reported previously in a patient (Vaina et al. 2003), further strengthening the view that processing for radial motion direction and speed occur at different spatial scales (Sekuler 1992; Morrone et al. 1995; Bex et al. 1998; Burr et al. 1998; Clifford et al. 1999).

By using a spatial summation paradigm we identified a systematic shift in the spatial scale over which speed and direction was processed. Following the loss in local motion sensitivity, WB's representation of motion direction and speed shifted to later stages of processing whose increased spatial integration of signals could be used to offset local motion deficits. In the case of speed discrimination this was later followed by a shift back to the use of local motion mechanisms and functional recovery on the task.

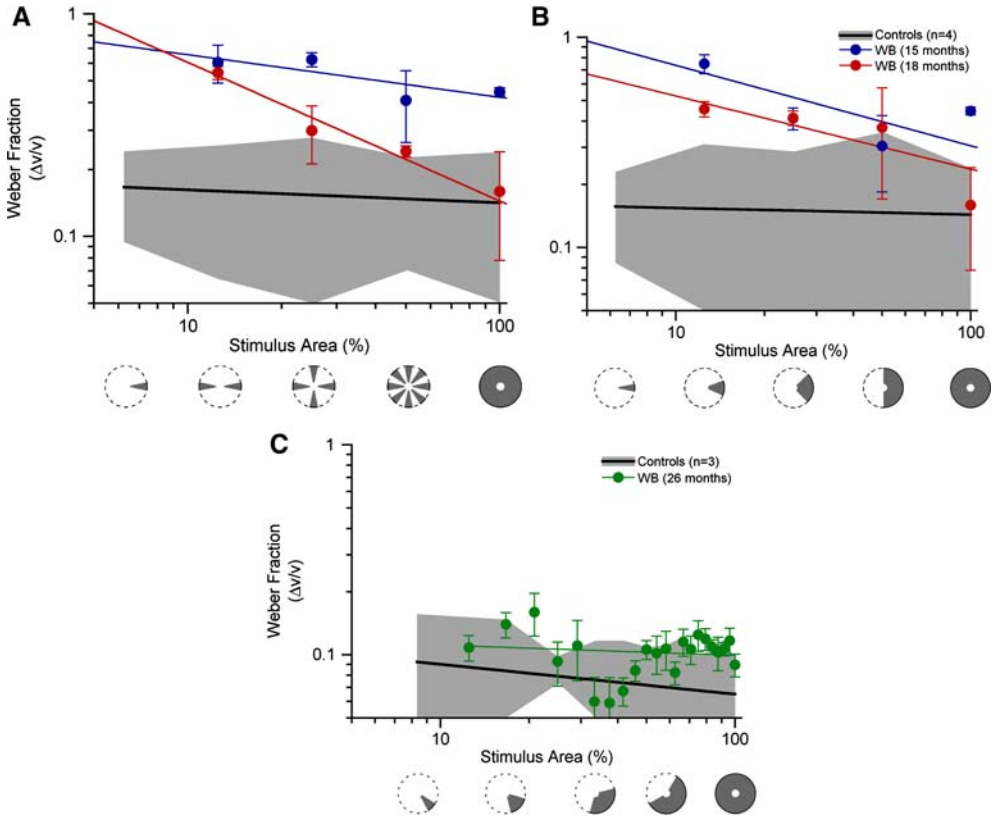

Fig. 6 Speed discrimination as a function of stimulus area. All symbols are the same as in Fig. 3. WB's speed discrimination was impaired 15 months after the lesion for both (**a**) multi- and (**b**) single-sector stimulus masks. Thresholds decreased linearly with stimulus area ($|\gamma| = 0.29 \pm 0.09$, $r^2 > 0.58$), contrasting sharply with normal observers who showed little or no effect of stimulus area ($|\gamma| = 0.04 \pm 0.03$). Spatial summation increased at 18 months ($|\gamma| = 0.49 \pm 0.14$) to levels predicted for an ideal observer ($|\gamma| = 0.5$), **c** twenty-six months after the lesion WB's ability to discriminate speed was normal for all mask conditions. WB's performance at this time showed no consistent effect of stimulus area resulting in little, if any, spatial summation ($|\gamma| = 0.05 \pm 0.08$)

For WB, the shift in summation mechanisms over time coupled with the significant effect of spatio-temporal integration for coherent radial motion provides strong evidence supporting the recruitment of higher-level radial motion mechanisms to process speed. However, the mechanisms mediating WB's functional recovery, and in particular the restoration of local motion processing, remain unclear. The shift from large to small spatial scales implied by the decrease in summation at 26 months suggests that those local motion mechanisms not lost following the stroke gradually recovered with time. Given the pattern in local versus global motion impairments, such recovery could reflect a top-down modulation of the remaining local motion mechanisms or a re-weighting of the inputs that feed into them. Each would act to restore function by increasing the gain of the remaining local motion mechanisms without requiring neural reorganization per se. This type of coarse gain modulation is consistent with the proposed role of cortical feedback projections in enhancing the feed forward activity that supports the global percept (Carpenter and Grossberg 1987; Mumford 1992; Lee and Mumford 2003; Raizada and Grossberg 2003; Deco and Lee 2004). Thus, existing feedback from higher cortical levels could be co-opted as a means to automatically guide functional recovery by systematically enhancing the remaining low-level mechanisms whose output has become degraded.

The combination of spatial summation as an experimental paradigm with longitudinal studies of patient performance provides an important window into the visual motion mechanisms that are disrupted following stroke and more importantly, the presence and coarse dynamics of recovery within those mechanisms. The shift in spatial scale of visual motion processing observed here suggests that deficits in low-level processing can be offset through the use of higher-level mechanisms that integrate low-level features across space. Computationally the use of spatial integration as a means to compensate uncertain or 'noisy' estimates from local mechanisms is reasonable. Thus, it is somewhat surprising that, in the case of speed at least, the visual system does not naturally utilize these more integrative information sources.

In contrast to the use of alternative visual cues or sources of information to facilitate functional recovery, the ability to shift processing to higher-level mechanisms presumes that the low-level processing in question is not completely lost. In such cases however, the potential to use spatio-temporal integration as a means to compensate for low-level deficits could provide an important new avenue for functional recovery in patients following stroke.

Acknowledgments This work was supported by National Institutes of Health grant 5R01EY007861-14 to LMV. We thank Paola Favaretto for helping with data collection. We also thank the subjects, especially WB, for their participation in this study.

References

Ahissar M, Hochstein S (2004) The reverse hierarchy theory of visual perceptual learning. Trends Cogn Sci 8:457–464

Beardsley SA, Vaina LM (2001) A laterally interconnected neural architecture in MST accounts for psychophysical discrimination of complex motion patterns. J Comput Neurosci 10:255–280
Beardsley SA, Vaina LM (2004) A functional architecture for motion pattern processing in MSTd. In: Thrun S, Saul L, Schölkopf B (eds) Advances in neural information processing systems 16. MIT Press, Cambridge, MA, pp 1451–1458
Beardsley SA, Vaina LM (2005a) How can a patient blind to radial motion discriminate shifts in the center-of-motion? J Comput Neurosci 18:55–66
Beardsley SA, Vaina LM (2005b) Psychophysical evidence for a radial motion bias in complex motion discrimination. Vision Res 45:1569–1586
Bex PJ, Makous W (1997) Radial motion looks faster. Vision Res 37:3399–3405
Bex PJ, Metha AB, Makous W (1998) Psychophysical evidence for a functional hierarchy of motion processing mechanisms. J Opt Soc Am A Opt Image Sci Vis 15:769–776
Burr DC, Morrone MC, Vaina LM (1998) Large receptive fields for optic flow detection in humans. Vision Res 38:1731–1743
Carpenter GA, Grossberg S (1987) A massively parallel architecture for a self-organizing neural pattern recognition machine. Comp Vis Graph Image Proc 37:54–115
Clifford CWG, Beardsley SA, Vaina LM (1999) The perception and discrimination of speed in complex motion. Vision Res 39:2213–2227
Deco G, Lee TS (2004) The role of early visual cortex in visual integration: a neural model of recurrent interaction. Eur J Neurosci 20:1089–1100
Deco G, Rolls ET (2004) A neurodynamical cortical model of visual attention and invariant object recognition. Vision Res 44:621–642
Deco G, Zihl J (2001) A neurodynamical model of visual attention: feedback enhancement of spatial resolution in a hierarchical system. J Comput Neurosci 10:231–253
Geesaman BJ, Qian N (1996) A novel speed illusion involving expansion and rotation patterns. Vision Res 36:3281–3292
Geesaman BJ, Qian N (1998) The effect of complex motion pattern on speed perception. Vision Res 38:1223–1231
Hahnloser RH, Douglas RJ, Hepp K (2002) Attentional recruitment of inter-areal recurrent networks for selective gain control. Neural Comput 14:1669–1689
Hatsopoulos NG, Warren WH (1991) Visual navigation with a neural network. Neural Netw 4:303–317
Hochstein S, Ahissar M (2002) View from the top: hierarchies and reverse hierarchies in the visual system. Neuron 36:791–804
Lee TS, Mumford D (2003) Hierarchical Bayesian inference in the visual cortex. J Opt Soc Am A Opt Image Sci Vis 20:1434–1448
Meese TS, Anderson SJ (2002) Spiral mechanisms are required to account for summation of complex motion components. Vision Res 42:1073–1080
Meese TS, Harris MG (2001) Independent detectors for expansion and rotation, and for orthogonal components of deformation. Perception 30:1189–1202
Morrone MC, Burr DC, Vaina LM (1995) Two stages of visual processing for radial and circular motion. Nature 376:507–509
Mumford D (1992) On the computational architecture of the neocortex. II. The role of cortico-cortical loops. Biol Cybern 66:241–251
Pelli DG (1997) The VideoToolbox software for visual psychophysics: transforming numbers into movies. Spat Vis 10:437–442
Perrone JA, Stone LS (1998) Emulating the visual receptive-field properties of MST neurons with a template model of heading estimation. J Neurosci 18:5958–5975
Raizada RD, Grossberg S (2003) Towards a theory of the laminar architecture of cerebral cortex: computational clues from the visual system. Cereb Cortex 13:100–113
Sekuler AB (1992) Simple-pooling of unidirectional motion predicts speed discrimination for looming stimuli. Vision Res 32:2277–2288
Tyler CW, Chen CC (2000) Signal detection theory in the 2AFC paradigm: attention, channel uncertainty and probability summation. Vision Res 40:3121–3144
Usher M, Niebur E (1996) Modelling the temporal dynamics of IT neurons in visual search: a mechanism for top-down selective attention. J Cogn Neurosci 8:311–327
Vaina LM, Gryzwacz NM, Saiviroonporn P, LeMay M, Bienfang DC, Cowey A (2003) Can spatial and temporal motion integration compensate for deficits in local motion mechanisms? Neuropsychologia 41:1817–1836
Watamaniuk SN, Duchon A (1992) The human visual system averages speed information. Vision Res 32:931–941
Watamaniuk SNJ, Sekuler R (1992) Temporal and spatial integration in dynamic random-dot stimuli. Vision Res 32:2341–2347
Zemel RS, Sejnowski TJ (1998) A model for encoding multiple object motions and self-motion in area MST of primate visual cortex. J Neurosci 18:531–547